2011 International Nuclear Atlantic Conference - INAC 2011
Belo Horizonte,MG, Brazil, October 24-28, 2011
Associação Brasileira de Energia Nuclear - ABEN
ISBN: 978-85-99141-04-5

COMPARISON AMONG TOMOGRAPHIC RECONSTRUCTION ALGORITHMS WITH A LIMITED DATA

Eric F. Oliveira[1], Sílvio B. Melo[2], Carlos C. Dantas[3], Daniel A. A. Vasconcelos[4] and Luís F. Cadiz[5]

[1]Department of Nuclear Energy -DEN
Federal University of Pernambuco – UFPE,
Av. Prof. Luiz Freire 1000, CDU 50740-540
Recife, PE, Brazil
efofisica@gmail.com

[2]Informatic Center - CIN
Federal University of Pernambuco – UFPE
Av. Prof. Luiz Freire 1000
CDU 50740-540 Recife, PE, Brazil
sbm@cin.ufpe.br

[3] Department of Nuclear Energy -DEN
Federal University of Pernambuco – UFPE,
Av. Prof. Luiz Freire 1000, CDU 50740-540
Recife, PE, Brazil
ccd@ufpe.br

[4]Department of Nuclear Energy -DEN
Federal University of Pernambuco – UFPE,
Av. Prof. Luiz Freire 1000, CDU 50740-540
Recife, PE, Brazil
azevedo.radiologia@gmail.com

[5]Department of Nuclear Energy -DEN
Federal University of Pernambuco – UFPE,
Av. Prof. Luiz Freire 1000, CDU 50740-540
Recife, PE, Brazil
luisfelipecadiz@hotmail.com

ABSTRACT

Nowadays there is a continuing interest in applying computed tomography (CT) techniques in non-destructive testing and inspection of many industrial products. These applications of CT usually require a differentiated analysis when there are strong limitations in acquiring a sufficiently large amount of projection data. The use of a low number of tomographic data normally degrades the quality of the reconstructed image, highlighting the formation of artifacts and noise. This work investigates the reconstruction methods most commonly used (FBP, ART, SIRT, MART, SMART) and shows the performance of each one in this limited scenario. For this purpose, all methods were implemented and tested with a phantom of uniform density with well-known distribution, with measures of transmission of gamma radiation in a first generation CT scanner. The phantom is a concentric stainless steel tube coupled with a half - cylinder of aluminum. The measurements were made with an

highest root mean square error, with the formation of visible artifacts. The artifacts are diminished but still visible in the ART and SIRT techniques, and the best performance was observed with the techniques MART and SMART. The technical superiority of these multiplicative methods is clearly seen in the reconstructed image quality, endorsing their application to situations of limited input data.

1. INTRODUCTION

There is continuing interest in the application of radiation techniques in non-destructive testing and inspection of many industrial products like steel plates produced by continuous casting, wood processing, nuclear cores reactor, integrated circuits and printed circuit boards. Computed tomography (CT) have allowed the generation of complete objects using the radiation data. With the rotation (scan) the entire radiation source-detector around the axis of an object, it is possible to quantify the attenuation suffered by the radiation in different directions (projections). The aim of tomography is to discover, from projection, the distribution of densities that internally represents an object. This distribution is represented as a function or image and to find it, the methods are used for reconstruction. These are divided into two classes: transformed or analytical methods and algebraic or interactive. Among the analysts, there is the algorithm of filtered backprojection (FBP), and between iterative has the algebraic reconstruction techniques additive correction (ART)and simultaneous (SIRT), algebraic reconstruction techniques multiplicative correction (MART) and simultaneous (SMART).

Because CT imaging has the medical industry as a driver in the 1970, most references are found in this area. On the other hand, in industries, applications of CT require a differentiated analysis [1], where in some situations may not be possible to acquire a large amount of projection data. Often it is impossible to surround with a ring of detectors an object as an airplane, for example. The use of a small number of tomographic data (projections) can lead to a reconstructed image of poor quality, which include the formation of artifacts and noise caused by insufficient information. Inconsistencies in data from the stochastic process of radioactive emissions and measures imposed by the fluctuations in equipment acquisition will also contribute to poor image quality. The aim of this study is to compare the five reconstruction algorithms mentioned, and which are widely used in CT, to pinpoint the most suitable for situations with a limited number of projection data. Aside from that, over the past years, few scientific studies have been performed in Brazil with this focus. The algorithms are evaluated using the Root Mean Square Error (RMSE) in the reconstruction of the distribution density of a half moon of aluminum in a stainless steel tube. The transmission range of measures are performed on a CT scan of the experimental arrangement with a third generation source of ^{137}Cs, scintillation detector NaI (Tl) and only 20 scans.

2. COMPUTED TOMOGRAPHY

Under the physical aspect, radiation to interact with a material can cause atomic or molecular excitation, ionization or activation of the nucleus. The X and gamma radiation are ionizing electromagnetic radiation of most interest for use in CT, because due to its wave nature, no charge and rest mass, can penetrate the material over great thickness before undergoing an interaction. The interaction of an electromagnetic wave with matter occurs in three ways:

photoelectric effect, Compton and pair production. The probability of the radiation beam interacting with matter through these processes is called the total attenuation coefficient of the material or linear (μ) when passing through a material (Figure 1), the intensity of the radiation suffers an exponential decay described by the Beer-Lambert relationship, equation 1.

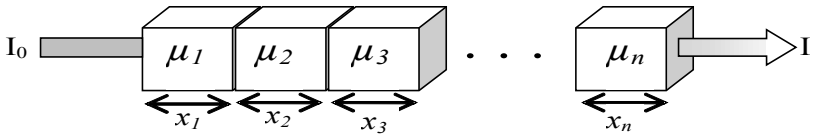

Figure 1: Attenuation of radiation by different attenuation coefficients

$$I = I_0 e^{-(\mu_1 x_1 + \mu_2 x_2 + \mu_3 x_3 + \ldots + \mu_n x_n)} \Leftrightarrow \sum_{n=1}^{N} \mu_n \cdot X_n = \ln \frac{I_0}{I} . \quad (1)$$

Where I is the final intensity of the radiation, I_0 the initial intensity of the radiation, the linear attenuation coefficient μ and X is the distance traveled by the ray. The $ln(I_0/I)$ is called one-dimensional projection of the body in the direction of the ray. On CT, the rotation (scan) the entire radiation source-detector around the axis of an object, record a series of projections resulting from rays passing through the same section in different directions.

3. TOMOGRAPHIC RECONSTRUCTION

After the scans, the radiating section of the object is treated as a function μ(x,y), which should be found by some method of reconstruction. Five techniques are displayed below.

3.1 Filtered Back Projection (FBP)

Bracewell and Riddle in 1967, introduced the method called filtered backprojetion (FBP) method based on Fourier Transform. The FBP is widely used due to low processing time. The theorem of projections, also called a center cut theorem (*Central Slice Theorem-CST*) facilitates the process. This says a 1D Fourier transform of the Radon transform of the function corresponds to 2D Fourier transform of the function. That is, performing the Fourier transform of the projections, one arrives at the space frequency distribution of densities that wish to discover. Within the operations are performed frequency filtering and 2D inverse transform returns the reconstructed image. The FBP is summarized in the following steps:

1. Calculate the Fourier transform one-dimensional projections of reaching the frequency domain.
2. Filter the projections transformed with a low pass filter (Shepp-Logan, Hann, Hamming, etc.).
3. Place the filtered projections in a polar grid. Each projection in its corresponding

angle.

4. Resample these in a Cartesian grid with interpolation (linear, nearest, splines, etc.).
5. Calculate the two-dimensional inverse Fourier transform, coming to the reconstructed image.

3.2 Algebraic Reconstruction Technique (ART)

Algebraic methods, or series expansion, discretized section radiated in a matrix of unknowns (pixels) representing the density distribution function μ(x,y) (Figure 2). After sweeps, a system of equations resulting from the Beer-Lambert relationship is created and its resolution matches the inverse Radon. Due to the characteristics of this system, indirect methods are advised, and among the indirect method of projections Kaczmarz has guaranteed convergence [2]. The iterative techniques are summarized basically in four steps: creation of the initial image, calculation of corrections, patches and application of the convergence test. These algorithms differ in how corrections are calculated and applied [3]. In his work, the algebraic technique is used ART. In this representation, a ray corresponds to a band width mostly coincides with the width of one pixel.

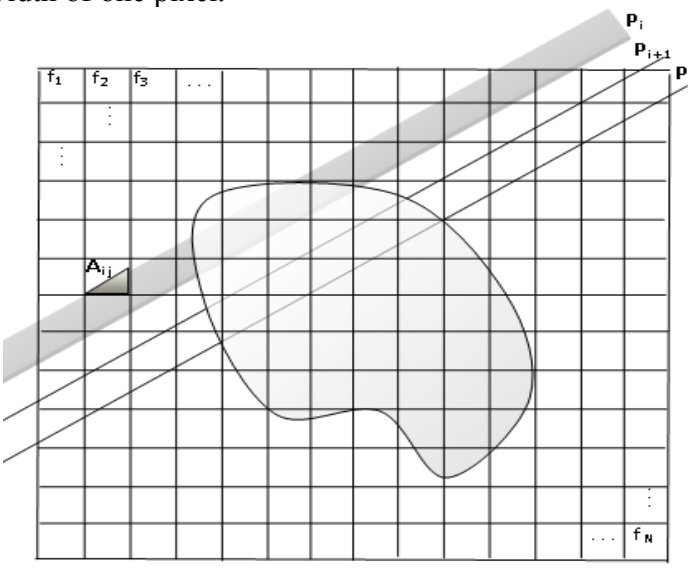

Figure 2: Discretization of the irradiated section

The process can be summarized in:

1) Create an initial image array with N elements parameterized j, usually radon or zero. This is the beginning of the 1st iteration (k=1).

2) Calculate the projections $P'(i)$ for all the rays from the formula:

$$\sum_{j=1}^{N} f'(j) \cdot w_{ij} = P_i' \qquad i = 1,2,3,...,M \tag{2}$$

3) For each ray i calculate the difference between the original projection $P(i)$ and rebuilt $P^{'}(i)$.

4) Calculate the sum of all weights along each ray.

$$W_i = \sum_{j=1}^{N} w_{ij}^2 \tag{3}$$

5) Get the fix for each ray i.

$$\alpha_i = \frac{\Delta P_i}{W_i} \tag{4}$$

6) Apply the patch to each cell j along the ray i.

$$f_k^{'}(j) = f_{k-1}^{'}(j) + \lambda \cdot w_{ij} \cdot \alpha_i \tag{5}$$

where λ is a relaxation parameter between 0 and 2.

7) Repeat steps 2-6 for all rays.

8) Find the sum of the convergence of all pixels in the image.

$$\Delta f = \sum_{j=1}^{N} \frac{f_{'}^{k} - f_{'}^{k-1}}{f_{'}^{k}}$$

9) End iteration k.

The iterations are terminated when Δf reaches a established. Many authors established a criterion $\Delta f \leq 0,01\%$. If the criterion was not met, a new iteration is initiated in step 2.

3.3 MART (Multiplicative Algebraic Reconstruction Technique with Correction)

Several studies point out the method as faster, more flexible and better accuracy than the ART. As indicated mainly in case of limited number of data [4]. The techniques is similar to ART, with change only in the correction factor expressed by equation 6, relative to the ray i.

$$\alpha_i = \frac{\Delta P_i}{P_i \cdot W_i} \tag{6}$$

3.4 SIRT (Simultaneous Algebraic Reconstruction Technique)

Although Gilbert in 1972 to have developed independently of the ART technique, the algorithm is similar, changing only the order in which corrections are applied. The corrections are found by the same procedure described in ART, but only the average of these

is applied (Equation 7) at the end of an iteration (Equation 8).

$$\alpha_{mj} = \frac{\sum_{i=1}^{n} \alpha_i}{n} \tag{7}$$

where n is the number of corrections found for the cell *j*.

$$f_k^{'}(j) = f_{k-1}^{'}(j) + \lambda \cdot \alpha_{mj} \tag{8}$$

3.5 SMART(Simultaneous Multiplicative Algebraic Reconstruction Technique with Correction)

It has the same advantages of MART and is also recommended for cases of a limited number of data [4]. The technique is similar to the SIRT, with change only in the correction factor expressed by equation 2-5 relative to the ray i.

$$\alpha_i = \frac{\Delta P_i}{P_i \cdot W_i} \tag{9}$$

4. METHODOLOGY

Phantoms are test objects with well defined distribution of densities that are used to evaluate the performance of the entire system of computing tomography. The sinogram is obtained through the acquisition of the object ad its tomographic cut should be rebuilt. The phantom used is a half moon of homogeneous aluminum in a stainless steel tube, also homogeneous, used to simulate a riser-type FCC-fluid catalitic cracking units- because the risers are very thick tubes made mostly of concrete and steel are widely used in the oil industry. In the riser, the range computed tomography has the task of finding properties, especially the flow and distribution of catalyst in the refining process for later use in the evolution of the process [5]. The aim of the experiment is to evaluate the performance of algorithms in the reconstruction of the distribution density of the half moon in the presence of steel pipe. The transmission range of measures are carried out with an experimental arrangement ^{137}Cs source, counts of 30s to 662 KeV photon energy in the scintillation detector Nal(Tl). 10mm collimation and 5.5mm at source on the detector.

Material characteristics: internal diameter of 15.4cm and 16.8cm external to the stainless steel tube, density of 7.9 g/cm³. For steel and aluminum; coefficient mass attenuation for 662 KeV gamma radiation is equal to 0.0762cm²/g for steel and 0.0777 cm²/g for aluminum.

12 scans are performed with step angle of 15 and 86 projections each with a 2mm linear step Xs. The procedure returns the matrix of intensity denoted tomogram 86x12 final size is equivalent to 1164 projections I. An arithmetic mean of the top 100 scores is performed for

the calculation of I_0 . The $\ln(I_0/I)/x_s$ is held for all returning sinogram projections to be used reconstruction. Negatives values are replaces by zero. The CT scanner with the tube shown in Figure 3.

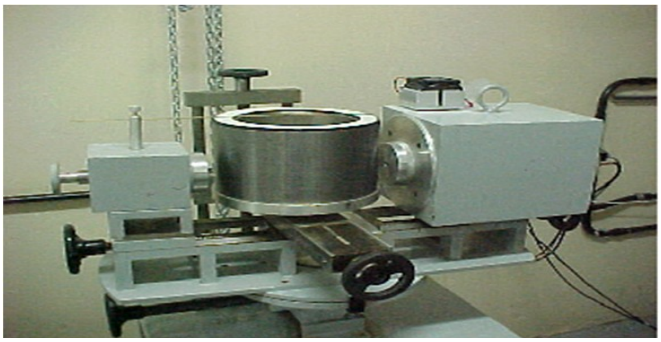

Figure 3: a single-source CT scanner and stainless steel tube.

Although there are many ways to evaluate errors in the reconstruction [2][4][6][7]. In the present study we chose to Root Mean Square Error (RMSE) between original and reconstructed sinogram. The appraiser estimates how much the figure is close to rebuilt original. The definition of the error is:

$$RMSE = \sqrt{\frac{\sum_{j=1}^{N}(f(j) - f'(j))^2}{\sum_{j=1}^{N} f(j)}} \tag{10}$$

Where, $f(j)$ is the original value of the pixel, $f'(j)$the reconstructed pixel and N the total number of image pixels or sinogram.

The function *iradon.m matlab 2010.a* software was used to perform there construction by FBP. The function offers the interpolations: linear, nearest, spline, pchip, and cubic v5 cubic, and filters: Ram-Lak, Shepp-Logan, Cosine, Hamming and Hann. Since the algebraic methods were implemented in C++ for better performance. These images were initialized to null and value for an additive to multiplicative. The relaxation parameter that offers the best compromise between convergence and low RMSE was used. The stopping criterion was set to 200 iterations enough so that all methods achieve a RMSE of 0.001 between the images of successive iterations. All reconstructed images are post-processed with the substitution of a negative valuer by zero.

5. RESULTS

The acquisition returns an array 97x12 of tomographic projections called tomogram. This is illustrated in Figure 4a two perpendicular views in Figure 4b.

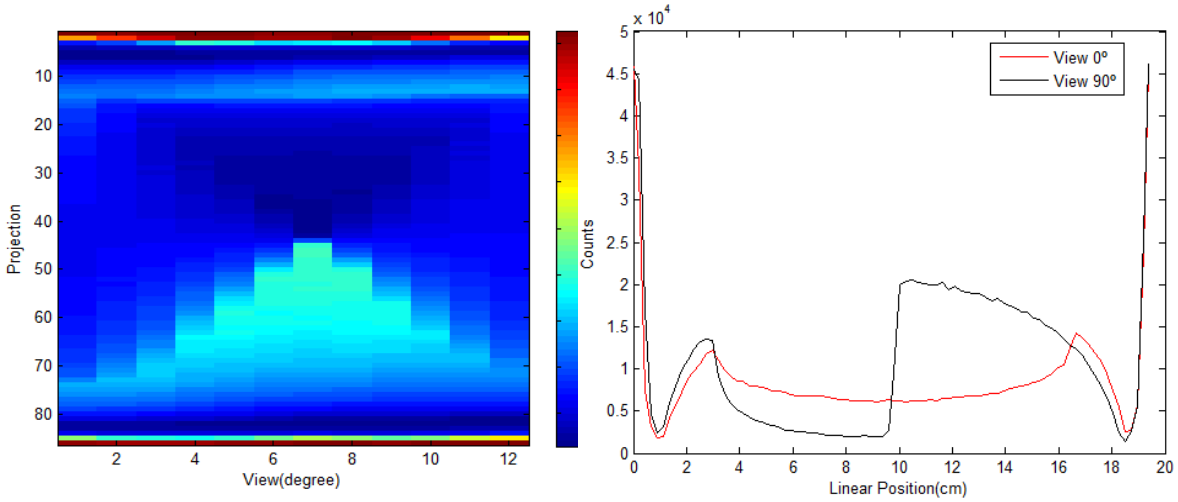

a) **b)**

Figure 4: a) Full Tomogram b) Two Perpendicular Views

With I_0 = 46550 counts calculate the sinogram is illustrated in Figure 5a, as well as two profiles in Figure 5b.

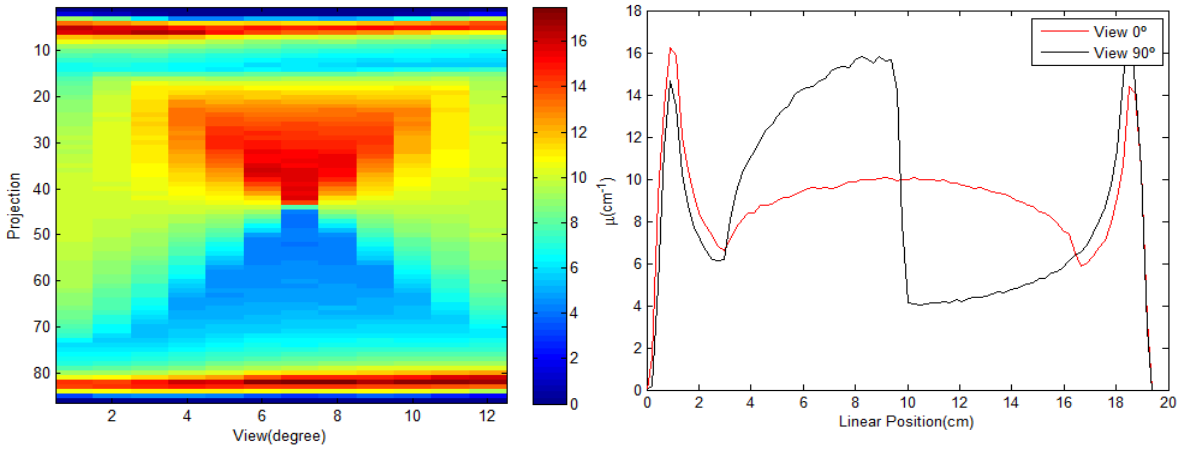

Figure 5: a)Sinogram with 12 views and 86 projections by view.

5.1 Filtered Back Projection

Were made every combination of interpolation filters provided by the software and offering the lowest error was the linear interpolation with Hann filter . This was 0.7796. The reconstructed image is illustrated in Figure 6a and two reconstructed profiles in Figure 6b.

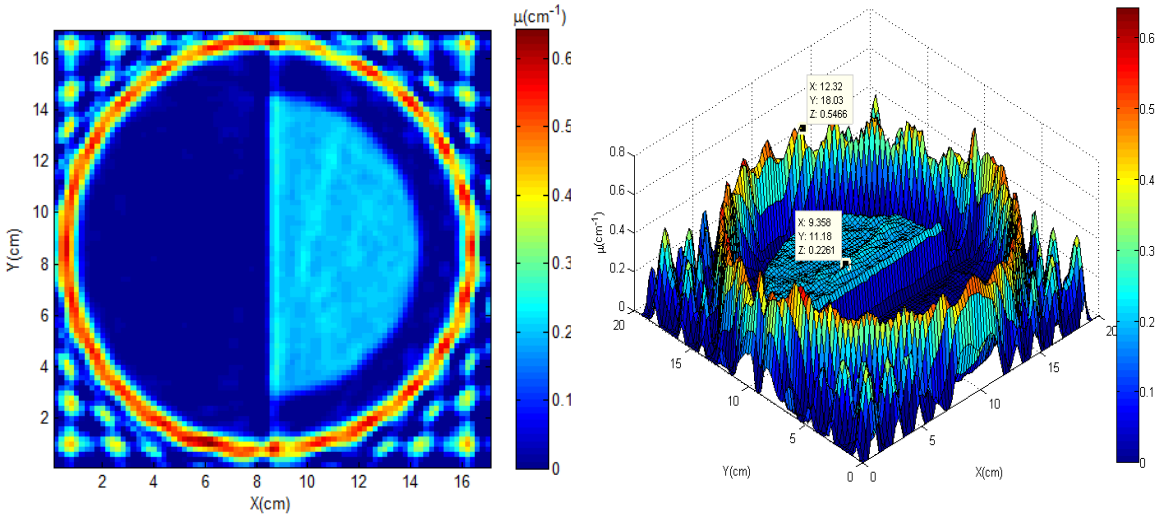

a)

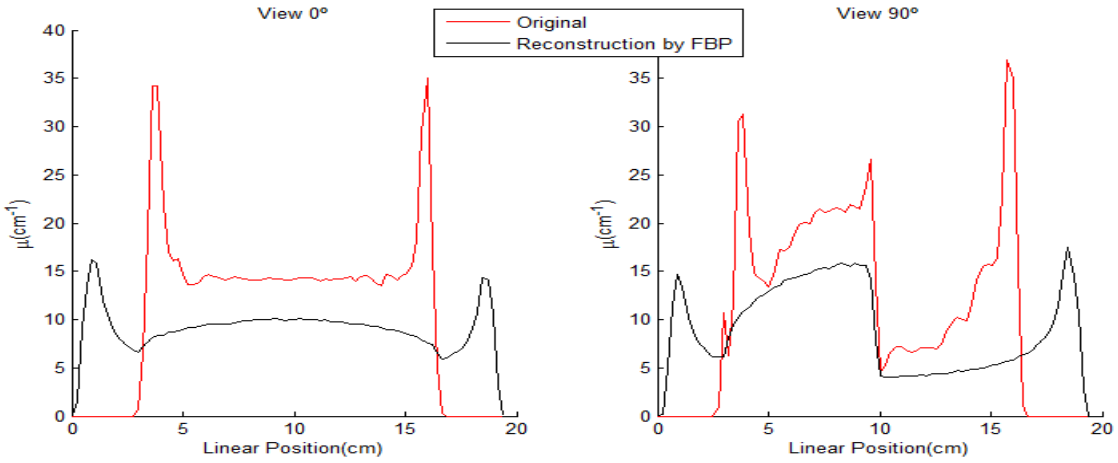

b)

Figure 6: Reconstructions by FBP. a) Reconstructed Image b) Views 0º e 90º

5.2 ART

The ralaxation parameter of 0.2 was used to achieve convergence after 100 iterations. Despite the still large number of artifacts found, these are smaller than the FBP, resulting in an RMSE of 0.09767.

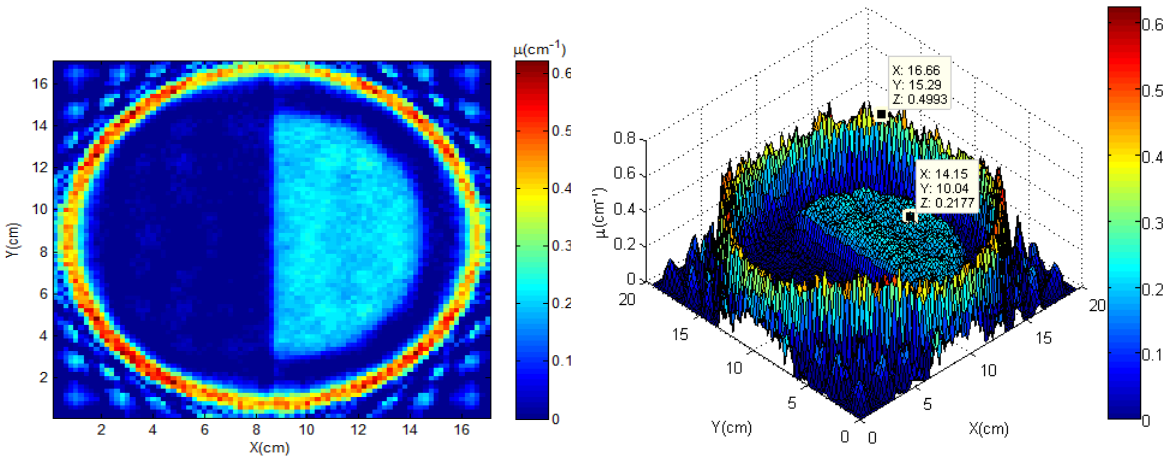

a)

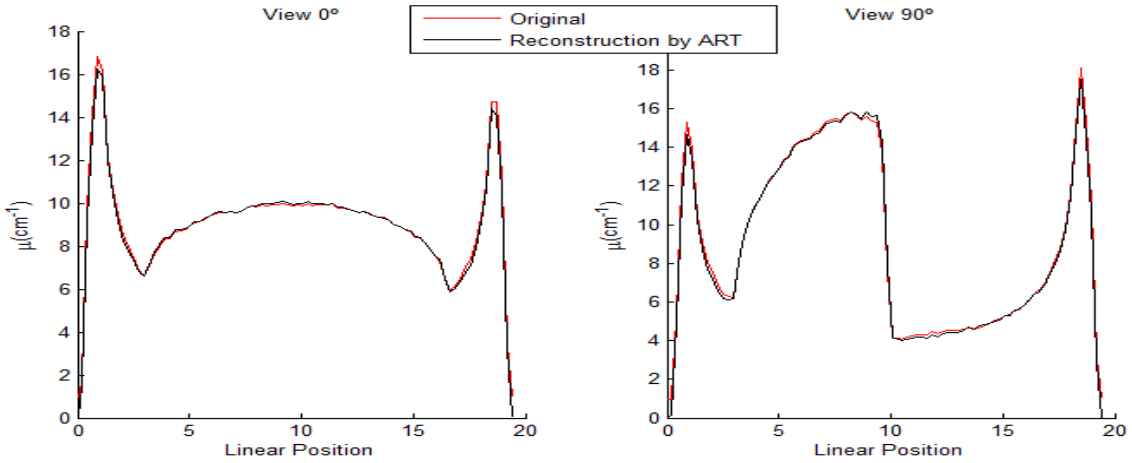

b)

Figure 7: Reconstructions by ART. a) Reconstructed Image b) Views 0º e 90º

5.3 MART

The relaxation parameter was 0.05. There is a considerable reduction of noise resulting in an RMSE of 0.01067.

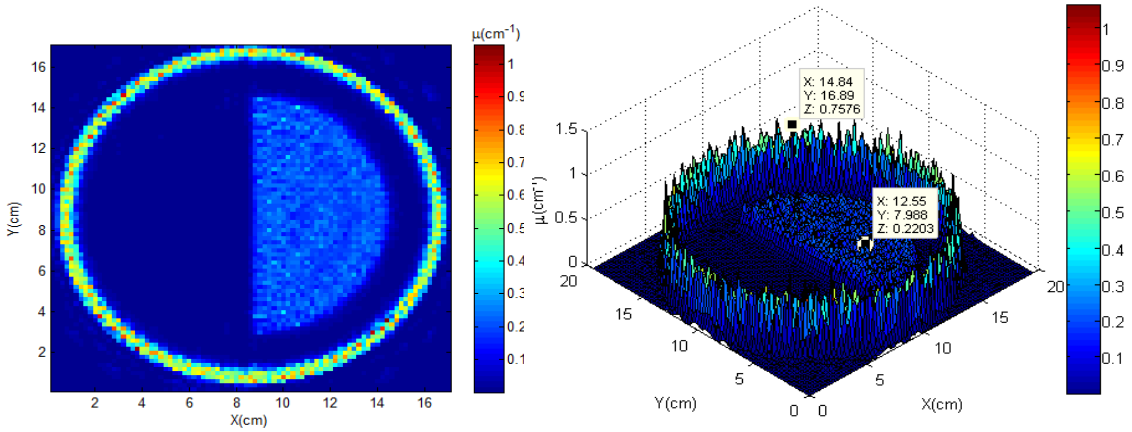

a)

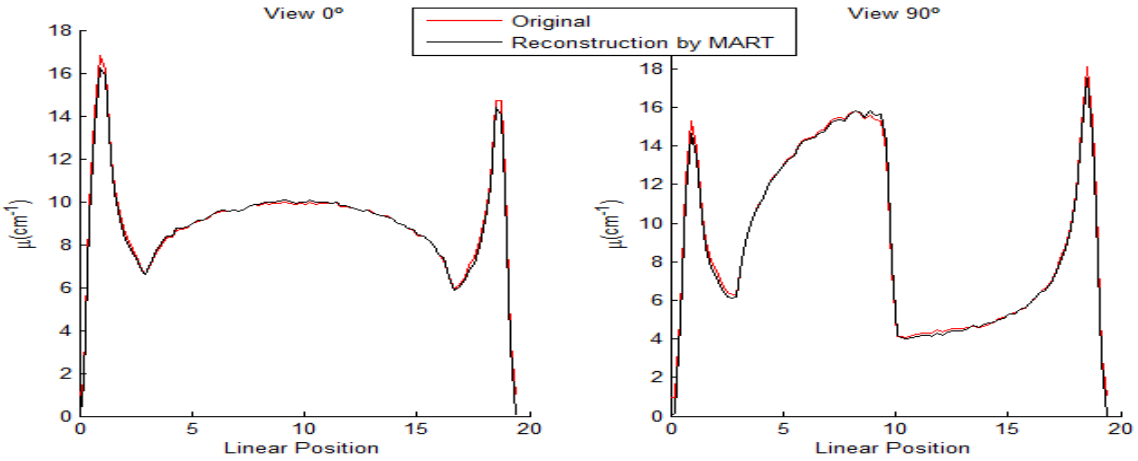

b)

Figure 8: Reconstructions by MART. a) Reconstructed Image b) Views 0º e 90º

5.4 SIRT

The relaxation parameter of 0.2 was used and obtained results similar to ART with a RMSE of 0.09767.

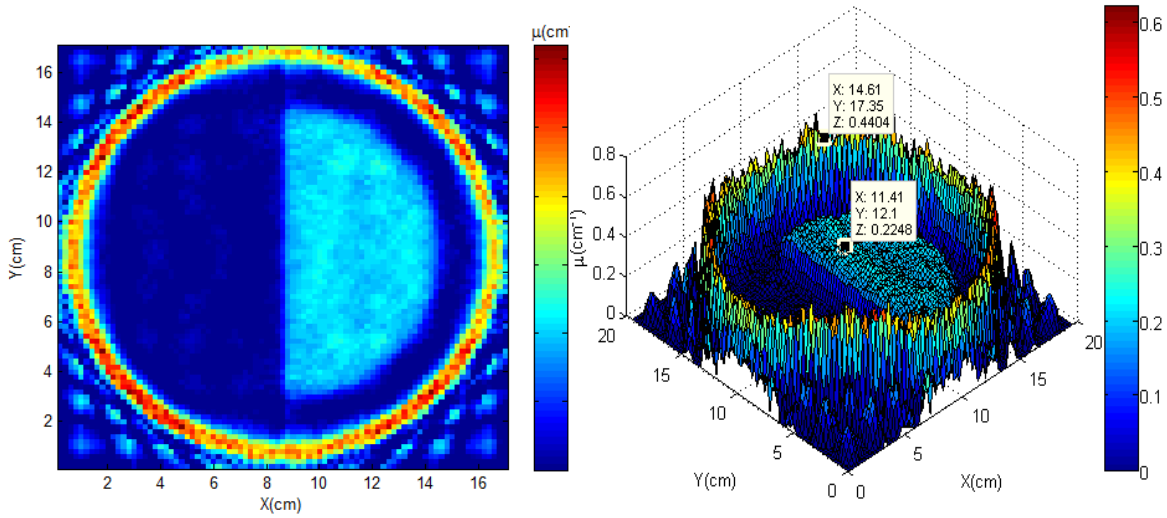

a)

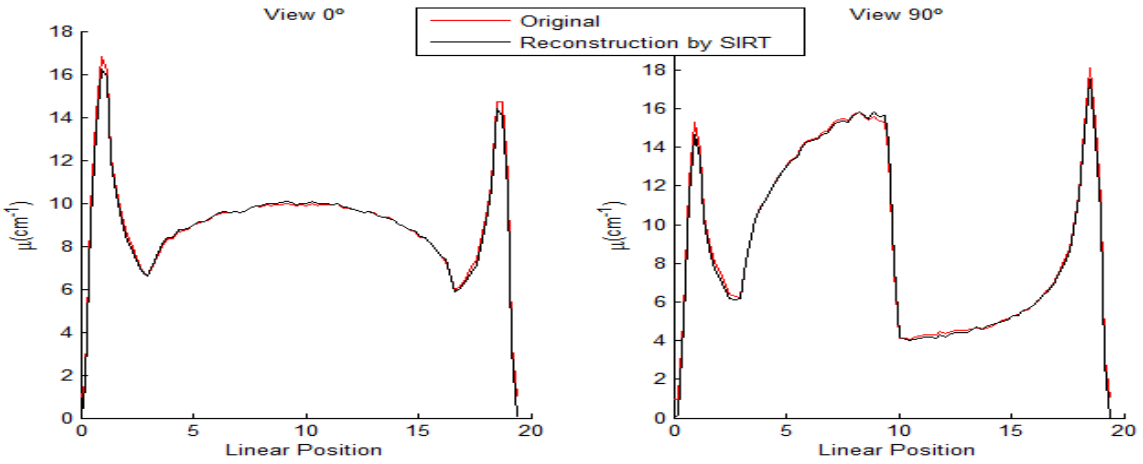

b)

Figure 9: Reconstructions by SIRT. a) Reconstructed Image b) Views 0º e 90º

5.5 SMART

The relaxation parameter was set at 0.03 and obtained a similar result to MART with RMSE of 0.01903.

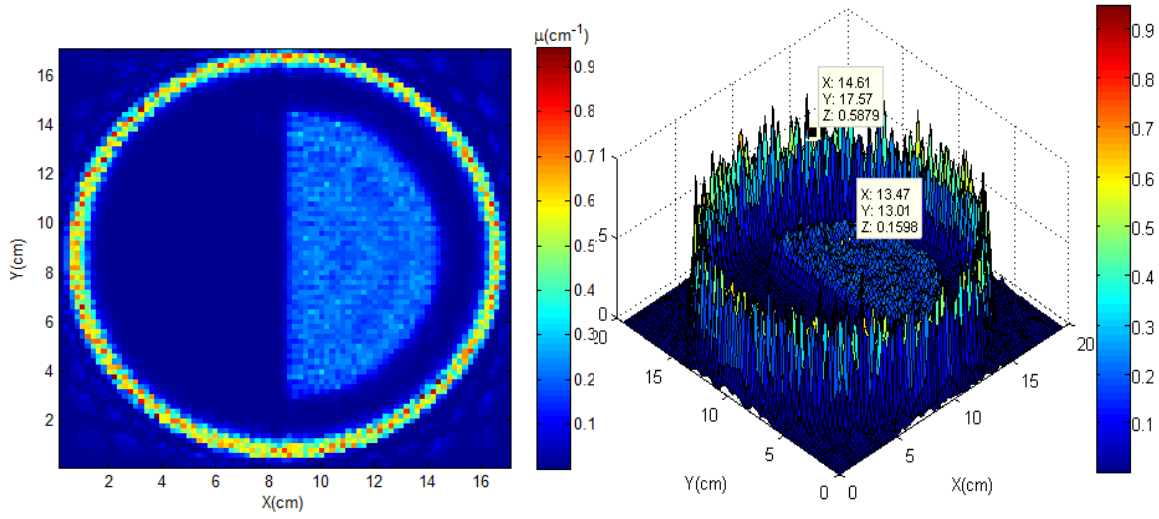

a)

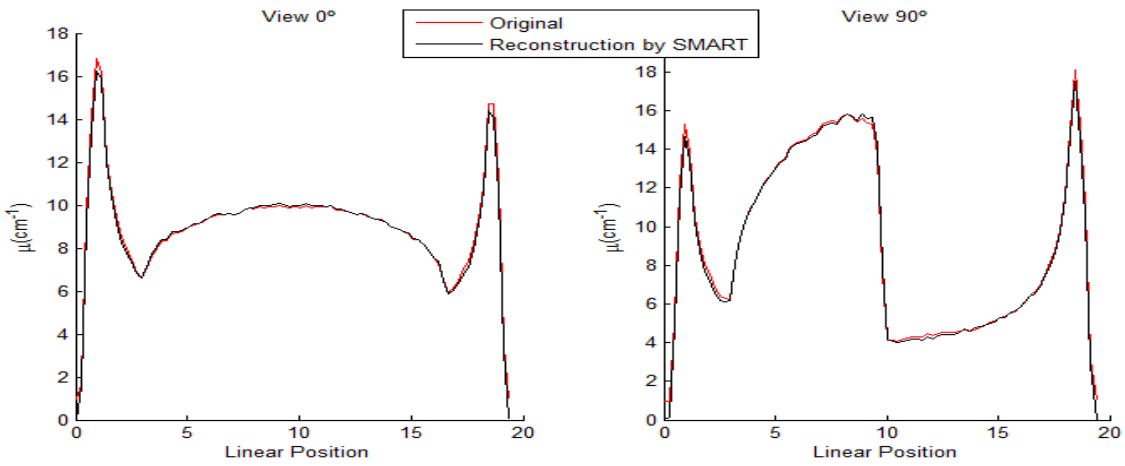

b)

Figure 10: Reconstructions by SMART. a) Reconstructed Image b) Views 0º e 90º

5.6 Convergence to Algebraic Reconstruction

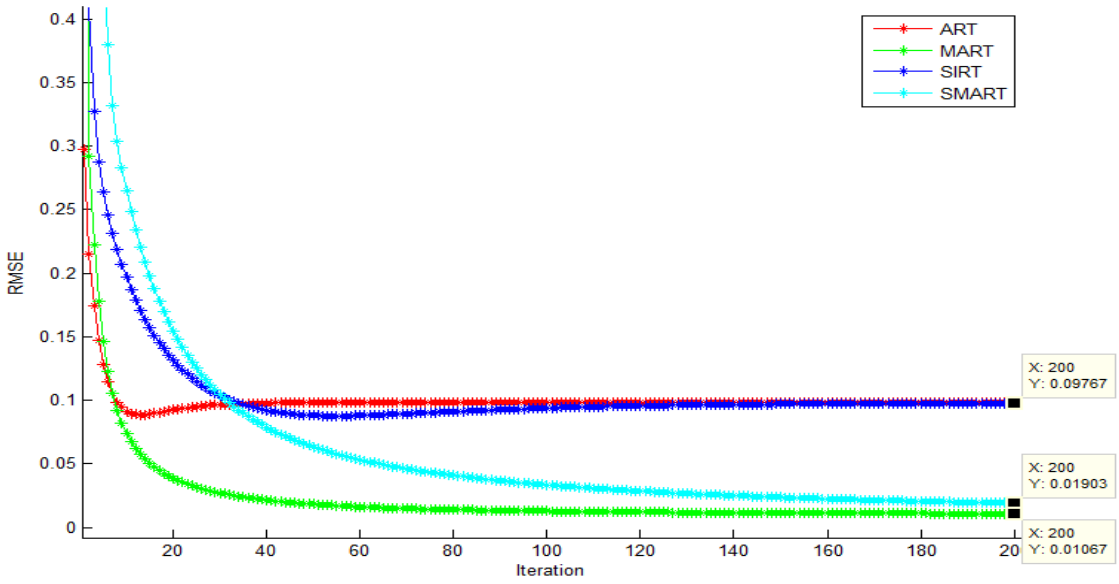

6. CONCLUSIONS

The algebraic reconstruction techniques were more efficient than the FBP technique transformed. This showed a large amount of noise, thus the highest RMSE. The algebraic techniques additive SIRT and ART is still noise, but in smaller numbers. Several authors [3] [4][8], algebraic techniques to recommend the limited data. According to KaK [9], the correction process in more susceptible to additive noise than the multiplicative techniques. This effect was observed and explains the difference of 8% for reconstructions multiplicative MART and SMART. They had the best performance, RMSE of 0.01067 to 0.01903 for

MART and SMART. This difference is hardly visible between the reconstructed images, since less than 5% differences between images are no easily perceived by the human eye [10]. Algebraic techniques have also achieved greater agreement between the original and reconstructed profiles.

ACKNOWLEDGMENTS

The financial support of CNPq and CAPES is greatly appreciated.

REFERENCES

1. SALVADOR, P. A. V., "Análise de sistemas multifásicos utilizando tomografia computadorizada gama monoenergética e polienergética", T*ese, IPEN-USP,* 2008.
2. KACZMARZ, S., "Angenaherte auflosung von systemen linearer gleichungen", *Bull. Acad. Pol. Sci. Lett. A*, vol. 6-8A, pp. 355-357 (1937).
3. SUBBARAO, P. M. V.; MUNSHI, P.; MURALIDHAR, K. Performance of iterative tomographic algorithms applied to non-destructive evaluation with limited data. *NDT & Internacional*, v.30(6), p.359–370, 1997.
4. VERHOEVEN D. Limited-data computed tomography algorithms for the physical sciences. *Applied Optics*, jul.,1993.
5. DANTAS, C.C. ; MELO,S.,M. ; OLIVEIRA, E. F. ; MAGALHÃES, F. P. ; SANTOS, M. G. "Measurement of density distribution of a cracking catalyst in experimental riser with a sampling procedure for gamma ray tomography". *Nuclear Instruments & Methods in Physics Research. Section B, Beam Interactions with Materials and Atoms (Print)* , v. 266, p. 841-848 (2008).
6. HERMAN, G. T.; GORDON, R. "Reconstruction of pictures from their projections. *Commun. Assoc. Comput. Mach*.", v14, p.759–768 (1971).
7. HERMAN, G. T. Iterative reconstruction algorithms. *Comput. Biol. Med.*, v6, p.273 – 294 (1976).
8. DE PIERRO, A. R. "Problemas Matemáticos em Tomografia por Emissão", Notas, UNICAMP (2004).
9. KAK, A. C.; SLANEY, M. "Principles of Computerized tomographic imaging", *IEEE PRESS*. 1999.
10. DE PIERRO, A. R. "Problemas Matemáticos em Tomografia por Emissão", Notas, UNICAMP (2004).